Supplement to:

Effects of sea ice cover on satellite-detected primary production in the Arctic Ocean

Mati Kahru[1], Zhongping Lee[2], B. Greg Mitchell[1] and Cynthia D. Nevison[3]

[1]Scripps Institution of Oceanography, University of California, San Diego, La Jolla, CA 92093, USA

[2]School for the Environment, University of Massachusetts Boston, Boston, MA 02125, USA

[3] University of Colorado, Boulder, Boulder, CO 80309, USA

1. Methods

We applied the quasi-analytic algorithm (Lee et al. 2002, 2005, 2009) to daily binned level-3 spectral remote sensing reflectance at ~9 km spatial resolution of multiple ocean colour sensors (OCTS, 1996-1997, version 2014.0; SeaWiFS, 1997-2010, version 2014.0; MERIS, 2002-2012, ESA 2nd processing; MODISA, 2002–2016, version 2014.0). As output from QAA we obtained the spectral absorption and backscattering coefficients at 440 and 490 nm wavelengths. We then merged the absorption coefficient at 490 nm (a490), coefficient of particulate backscattering (bbp490) and absorption coefficient due to phytoplankton at 440 nm (aph44) from different sensors and composited over 5-day periods.

Daily average photosynthetically active radiation (PAR, Frouin et al. 2003) was derived by merging binned 9-km datasets from all available sensors (OCTS, SeaWiFS, MODIS-Terra, MODIS-Aqua, VIIRS) and additional filling of gaps and extending coverage poleward using an empirical relationship between PAR and surface incoming shortwave (SIS) irradiance (Fig. 1) from geostationary and polar orbiting satellites (Mueller et al., 2009, Müller et al., 2015). SIS data were obtained from the Satellite Application Facility on Climate Monitoring (CM SAF, http://www.cmsaf.eu/EN/Products/AvailableProducts/Dataset/Dataset_node.html). While daily estimates of the merged PAR (Fig. 2) typically reached full coverage of the ice-free ocean area, in-water estimates were often limited by clouds. Even the 5-day composites of a490, bbp490 and aph440 had large areas of missing data. The relative proportion of valid data was increased by binning the ~9-km data to a grid of 0.25 degrees (~27 km). Temporal interpolation between neighbouring 5-day composites was used to fill some of the missing pixels. Spatial interpolation was used to fill remaining missing neighbouring pixel values. The interpolation and extrapolation operations were applied only if the corresponding 5-day mean ice fraction was below 15%. Sea-ice coverage was obtained from NASA Team algorithm datasets (version 1.1, http://nsidc.org/data/nsidc-0051.html) derived from passive microwave data.

As PAR conditions can change rapidly, even during the day, merging PAR estimates from multiple sensors with different measurement times increases the representativeness of the estimates of the mean daily PAR. In-water properties are expected change slower than PAR. Therefore, daily estimates of NPP were created from daily PAR and 5-day composites of in-water bio-optical properties. As input to the Vertically Generalized Production Model (VGPM, Behrenfeld and Falkowski 1997) we used Chla derived from phytoplankton

absorption at 440 nm (Bricaud et al 1998), merged PAR, depth of the euphotic zone calculated from a490 and bbp490 (Lee et al. 2007) and daily sea-surface temperature (SST). SST is known to have only a weak influence on NPP, therefore we used the optimally interpolated sea-surface temperature (Reynolds et al. 2007) that has no gaps. Daily NPP estimates were further composited into 5-day periods by averaging valid data during each 5-day period. NPP for pixels that had valid PAR, no ice (Cavalieri et al. 1996) but no ocean colour data after interpolation and extrapolation was calculated assuming a low Chla value (0.1 mg m^{-3}) with the estimated PAR. The effect of this assumption on the total annual NPP was very small (<1%) due to the typically very low PAR (due to low sun elevation and short period of daylight) at these high latitudes.

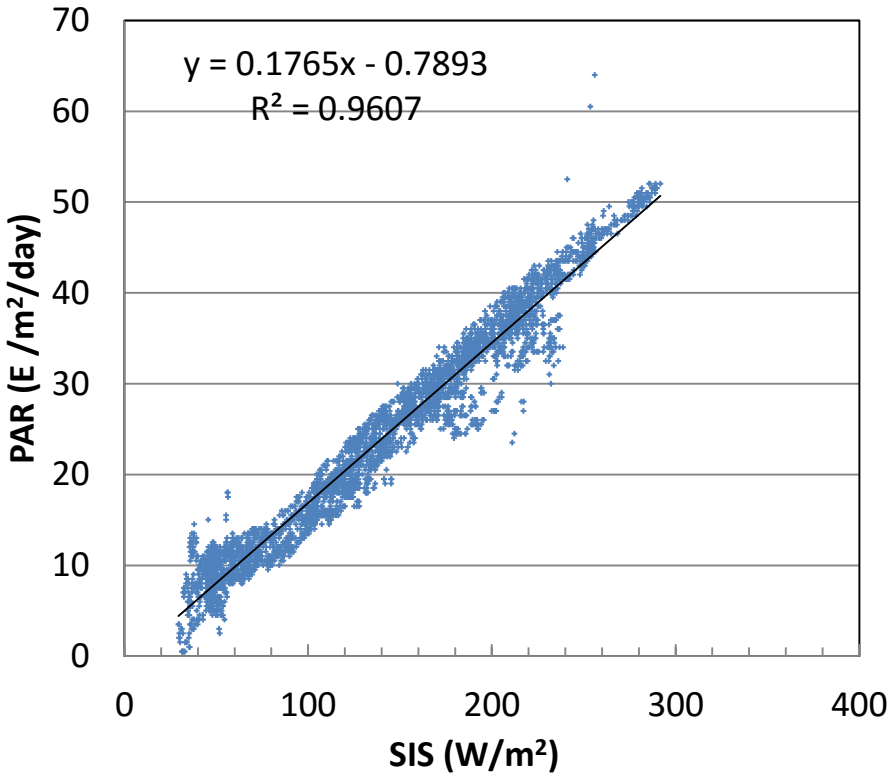

Figure 1. Empirical relationship between PAR and surface incoming shortwave (SIS) irradiance (SARAH dataset) from geostationary satellites (Mueller et al., 2009, Müller et al., 2015).

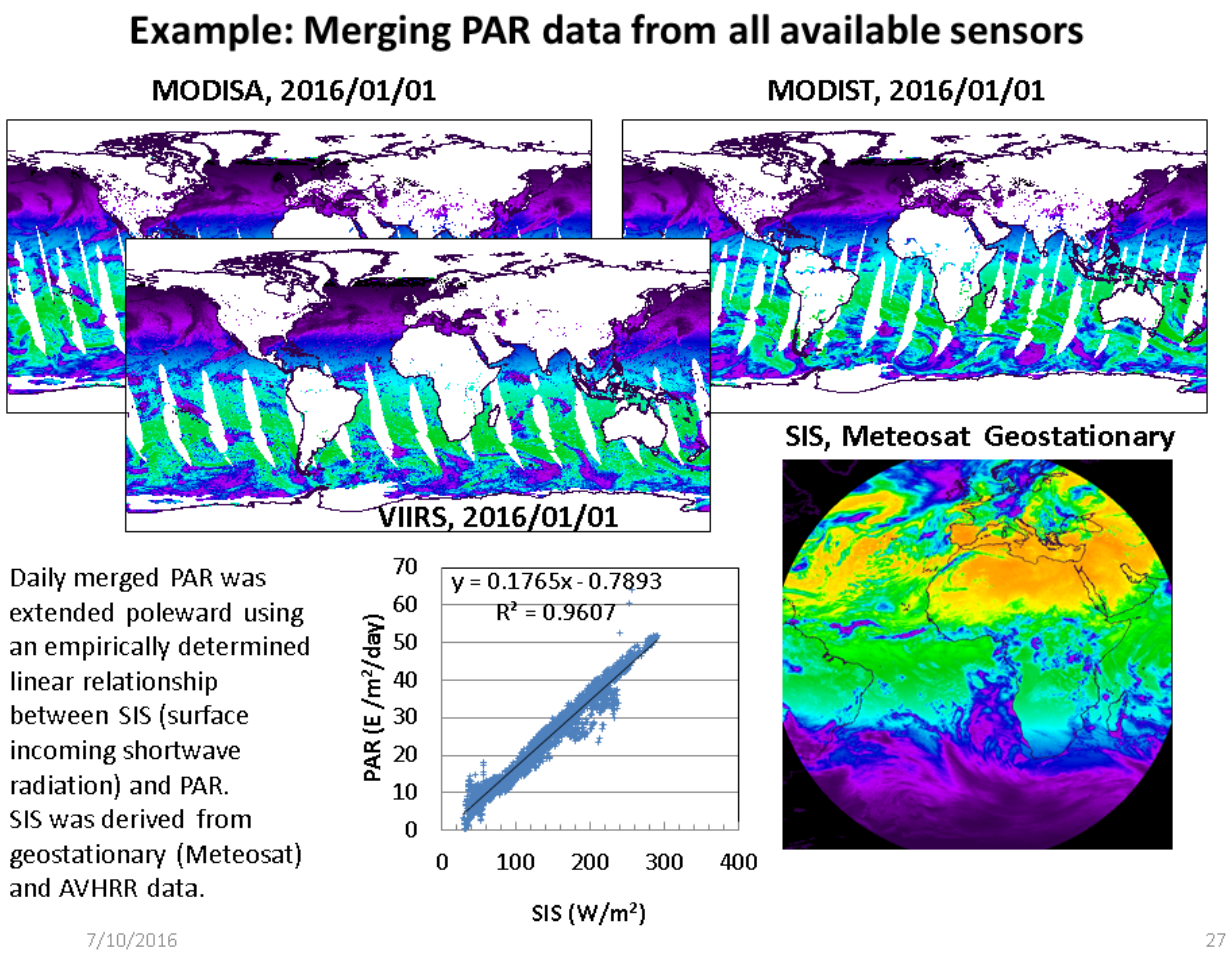

Figure 2. Example of merging PAR data for January 1, 2016 using PAR estimates of MODIS-Aqua, MODIS-Terra, VIIRS and additionally from Meteosat. Areas of missing data between the swaths of each sensor are filled by data from other sensors.

2. Processed satellite data

Processed satellite data used in this analysis are available online in 2 separate zipped files, respectively for periods 1997-2012 and 2013-2013. These files have series of 5-day global NPP datasets in HDF4 format (Kahru et al., 2016) and are available from the Dryad Digital Repository (http://dx.doi.org/10.5061/dryad.34f4q).

3. Validation

Limited validation of the combined methods involving both the NPP model itself and the process of interpolation and extrapolation has been done by comparing the derived NPP data with in situ data collected by the Palmer LTER program (Fig. 3). As a comparison, we also extracted match-ups from the well-known

NPP datasets produced by Oregon State University (M. Behrenfeld): the Carbon-based Productivity Model (CbPM, Behrenfeld et al. 2005, Westberry et al. 2008) and the Vertically Generalized Productivity Model (VGPM, Behrenfeld and Falkowski 1997), both using MODIS-Aqua 8-day composites as input. These datasets were downloaded from http://www.science.oregonstate.edu/ocean.productivity/. This limited and preliminary comparison shows that our model performs reasonably well while the CbPM has the lowest R^2 that is probably due to problems with some of its input variables, e.g. the mixed layer depth.

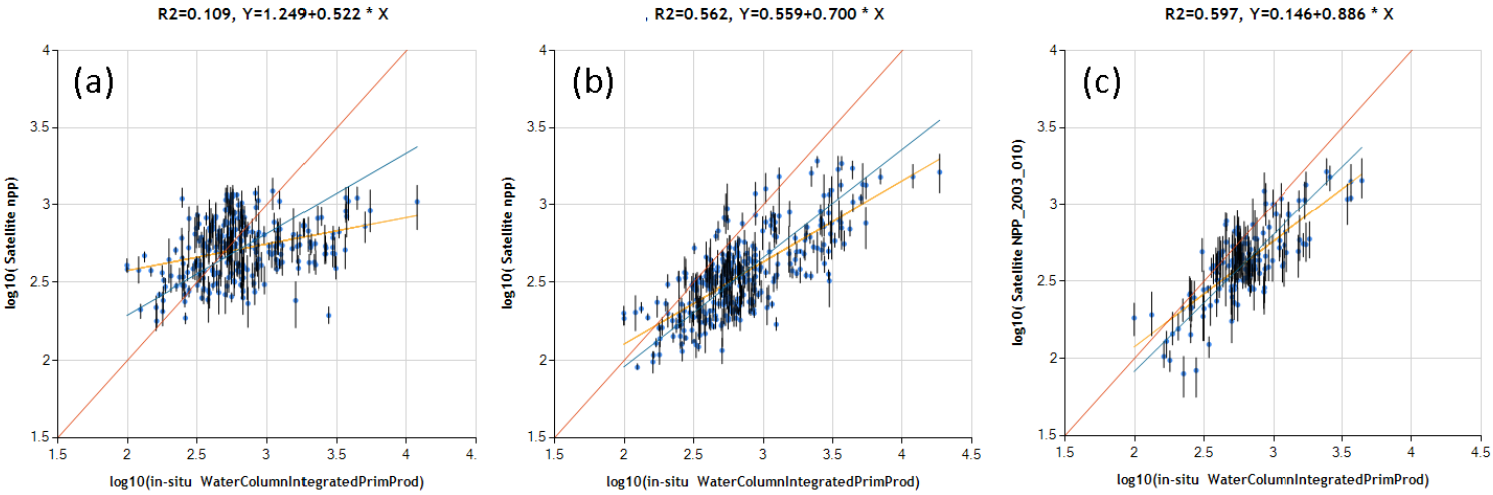

Figure 3. Match-ups of satellite-derived NPP versus *in situ* measured NPP by the Palmer LTER program using (*a*) Carbon-based Productivity Model (CbPM, Behrenfeld et al. 2005, Westberry et al. 2008), (*b*) Vertically Generalized Productivity Model (Behrenfeld and Falkowski 1997) and (*c*) NPP model described in this work. Red line shows the one-to-one relationship, blue dots are the satellite means for 3x3 pixel windows cantered at the nearest pixel and the vertical lines show the extent to variability inside the satellite 3x3 pixel area.

4. Results

Annual NPP as well as the summer monthly maximum as well as the summer mean NPP per area are summarized in Table 1.

Table 1. Summary of the estimated NPP in the Arctic Ocean between 66 ˚N and 84 ˚N for 1998-2015.

Period	Year	Annual NPP, PgC	Maximum monthly NPP, Pg C	NPP/area, mgC/m^2/day
Period 1	1998	0.347	0.082	622

	1999	0.369	0.093	559
	2000	0.385	0.092	565
	2001	0.384	0.093	514
	2002	0.436	0.110	522
	2003	0.444	0.105	731
	2004	0.477	0.106	671
	2005	0.488	0.120	561
	2006	0.492	0.108	614
Period 2	2007	0.566	0.149	601
	2008	0.512	0.133	632
	2009	0.528	0.137	608
	2010	0.611	0.147	447
	2011	0.675	0.154	469
	2012	0.698	0.154	499
	2013	0.691	0.160	487
	2014	0.656	0.151	461
	2015	0.669	0.152	463

References

Behrenfeld MJ, Falkowski PG. 1997 Photosynthetic rates derived from satellite based chlorophyll concentration, *Limnol. Oceanogr*., **42**, 1-20.

Behrenfeld MJ, Boss E, Siegel DA, Shea DA. 2005 Carbon-based ocean productivity and phytoplankton physiology from space. *Glob. Biogeochem. Cycles* 19:GB1006, doi:10.1029/2004GB002299.

Bricaud A, Babin M, Morel A, Claustre H. 1995 Variability in the chlorophyll-specific absorption coefficients of natural phytoplankton: Analysis and parameterization. *J. Geophys. Res*., **100**, 13321-13332.

Cavalieri DJ, Parkinson CL, Gloersen P, Zwally H. 1996 Updated yearly. Sea ice concentrations from Nimbus-7 SMMR and DMSP SSM/I-SSMIS Passive Microwave Data. Boulder, Colorado USA: NASA National Snow and Ice Data Center Distributed Active Archive Center.

Frouin R, Franz BA, Werdell PJ. 2003 The SeaWiFS PAR product, In Algorithm Updates for the Fourth SeaWiFS Data Reprocessing, ed. by S. B. Hooker and E. R. Firestone, NASA/TM-2003-206892, 22.

Lee ZP, Weidemann A, Kindle J, Arnone R, Carder KL, Davis C. 2007 Euphotic zone depth: Its derivation and implication to ocean-color remote sensing. *J. Geophys. Res.*, ***112***, C03009. (doi:03010.01029/02006JC003802)

Kahru M, Lee Z, Mitchell BG, Nevison CD. 2016 Effects of sea ice cover on satellite-detected primary production in the Arctic Ocean. Dryad Digital Repository. doi:10.5061/dryad.34f4q.

Mueller R, Matsoukas C, Gratzki A, Behr H, Hollmann R. 2009 The CM-SAF operational scheme for the satellite based retrieval of solar surface irradiance - A LUT based eigenvector hybrid approach, *Remote Sens. Environ.*, 113, 1012–1024.

Müller R, Pfeifroth U, Träger-Chatterjee C, Cremer R, Trentmann J, Hollmann R. 2015 Surface Solar Radiation Data Set - Heliosat (SARAH), Satellite Application Facility on Climate Monitoring, doi:10.5676/EUM_SAF_CM/SARAH/V001.

Westberry T, Behrenfeld MJ, Siegel DA, Boss E. 2008 Carbon-based primary productivity modeling with vertically resolved photoacclimation, *Global Biogeochem. Cycles*, 22, GB2024, doi:10.1029/2007GB003078.